

TABLE I. Comparison of deformation-potential constants $D_u^{a'}$ and $D_{ud}^{a'}$.

$D_u^{a'}$ (eV)	$D_{ud}^{a'}$ (eV)
2.2 ± 0.3^a	4.7 ± 0.4^a
2.1 ± 0.3^b	3.4 ± 0.4^b
1.9 ± 0.4^c	4.9^d

^aPresent result for *p*-Ge14.^bPresent result for *p*-Ge16.^cRef. 17.^dRef. 13.

determined separately, from fitting of the curves [Figs. 1(a) and 1(b)] along the abscissa and the ordinate, respectively. The static deformation-potential constant obtained here is very close to the one determined from the piezospectroscopic effect,¹² while the dynamic one is close to the value obtained from thermal conductivity measurements.⁸ The present results reconcile, therefore, the apparent discrepancy in the two values obtained from measurements in the two regimes $a^*q \ll 1$ and $a^*q \gtrsim 1$. These results are summarized in Table I.

The authors thank Dr. N. Mikoshiba and Dr. K. Suzuki for communicating their results^{10,13} prior to publication, and Mr. I. Gerstein for use of the stressing apparatus.

*Research supported in part by the National Science

Foundation and the Advanced Research Projects Agency.

†National Aeronautics and Space Administration International University Fellow, on leave of absence from Electrotechnical Laboratory, Tanashi, Tokyo, Japan.

¹W. Kohn, in *Solid State Physics*, edited by F. Seitz and D. Turnbull (Academic, New York, 1957), Vol. 5, p. 300.

²R. J. von Gutfeld, in *Physical Acoustics*, edited by W. P. Mason (Academic, New York, 1968), Vol. 5, p. 233.

³B. Taylor, H. J. Maris, and C. Elbaum, *Phys. Rev. B* **3**, 1462 (1971).

⁴Identical experiments were carried out on Si over a larger range of acceptor concentration. It was found that for sufficiently low acceptor concentration the application of stress has no effect on the amplitude of the transmitted phonons. For higher acceptor concentration the stress dependence has features similar to those found in Ge.

⁵V. Narayanamurti, *Phys. Lett.* **30A**, 521 (1969).

⁶It is noted that the corresponding minimum in Si shifts clearly to higher stress with increasing power input. These observations will be discussed further in a forthcoming paper.

⁷K. Suzuki, M. Okazaki, and H. Hasegawa, *J. Phys. Soc. Jap.* **19**, 930 (1964).

⁸K. Suzuki and N. Mikoshiba, *Phys. Rev. B* **3**, 2550 (1971).

⁹P. C. Kwok, *Phys. Rev.* **149**, 666 (1966).

¹⁰K. Suzuki and N. Mikoshiba, to be published.

¹¹M. J. Holland, *Phys. Rev.* **132**, 2461 (1963).

¹²R. I. Jones and P. Fisher, *Phys. Rev. B* **2**, 2016 (1970).

¹³N. Mikoshiba and K. Suzuki, private communication.

Generation and Detection of Large-*k*-Vector Phonons

M. J. Colles* and J. A. Giordmaine

Bell Telephone Laboratories, Murray Hill, New Jersey 07974

(Received 24 June 1971)

We report observations in diamond of buildup of acoustic phonons well out in the Brillouin zone. The acoustic phonon generation accompanies strong pumping by harmonic $k \approx 0$ optical phonons. Phonons are detected by their effect on impurity fluorescence. The Orbach phonon breakdown mechanism is calculated to play an important role.

In this Letter we report experiments in diamond in which the injection of $k \approx 0$ optical phonons at 1332 cm^{-1} by a stimulated Raman technique is observed to be accompanied by intense lattice excitation near half the optical phonon frequency. Both the optical phonons and subharmonic excitation are detected by strong hole burning in the spectrum of anti-Stokes fluorescence from localized impurity centers, a phenomenon not pre-

viously reported. We attribute the subharmonic excitation to decay of injected optical phonons into pairs of oppositely directed acoustic phonons with large k vector ($4 < \lambda < 9 \text{ \AA}$). The subharmonic phonons are observed under conditions for which coherent parametric phonon generation¹ is expected to be significant.

The experiments were carried out at 77°K in natural diamond crystals (type I) selected for

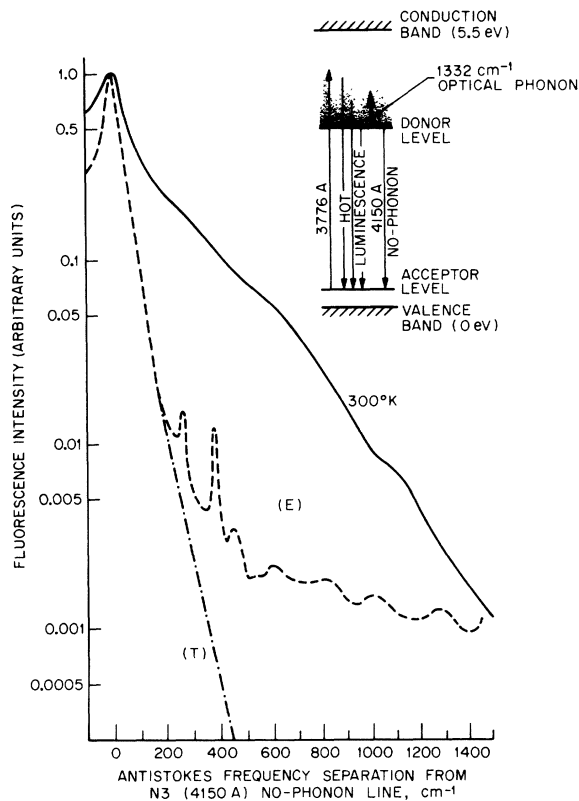


FIG. 1. Diamond N_3 -center anti-Stokes fluorescence at 300 and 77°K. Curve E is measured at 77°K; curve T is thermal-equilibrium fluorescence calculated from measured 77°K Stokes fluorescence spectrum. Inset is schematic one-electron energy-level scheme.

strong N_3 impurity-center fluorescence. This center has been identified as a substitutional, nearest-neighbor, nitrogen-aluminum pair,^{2,3} and has a sharp no-phonon transition at 4150 Å (frequency ν_0) corresponding to recombination of an exciton bound at the ionized donor-acceptor pair⁴ (Fig. 1, inset). The prominent phonon-assisted Stokes fluorescence continuum (and mirror-image anti-Stokes absorption) displays several broad one- and two-phonon maxima comparable to the no-phonon line in intensity.^{2,5} The expected thermal intensity ratio of anti-Stokes ($\nu_a > \nu_0$) to Stokes ($\nu_s = 2\nu_0 - \nu_a$) fluorescence is $R(\nu_a, T) = \exp[\hbar(\nu_a - \nu_0)/kT]$.

The observed anti-Stokes fluorescence of a strongly N_3 -luminescent diamond (specimen C_2) excited by 3663-Å Hg light is shown in Fig. 1. The 300°K spectrum is in satisfactory agreement with the 300°K Stokes spectrum multiplied by the thermal ratio $R(\nu_a, T)$. On the other hand, the 77°K spectrum shows a broad nonthermal "background" with a branching ratio of $\sim 2 \times 10^{-3}$ of the

no-phonon intensity, in excess of the level calculated from the Stokes spectrum and $R(\nu_a, T)$. This nonthermal background is attributed below to hot luminescence.^{6,7} At the frequency $\nu_0 + 1332 \text{ cm}^{-1}$ of $k \approx 0$ optical phonon-assisted fluorescence, the 77°K background has an intensity equivalent to thermal fluorescence at 270°K. It was verified that extraneous contributions from stray light and other sources were $< 20\%$ of the background level. In two other specimens, C_3 and C_4 having ~ 20 and 10% the N_3 fluorescence of C_2 , respectively, and our only other available specimens having N_3 fluorescence adequate for low-level measurement, we observed the same background to no-phonon ratio, as for C_2 . With pulsed 3776-Å excitation at 77°K the lifetimes⁸ of the fluorescence at ν_0 and at $\nu_0 + 1332 \text{ cm}^{-1}$ were $\leq 10^{-8}$ sec; the background fluorescence was a linear function⁸ of 3776-Å power for excitation intensities up to 10^6 W cm^{-2} .

Pump phonons at $\nu_p = 1332 \text{ cm}^{-1}$ were injected by driving⁹ the optical branch at $k \approx 0$ by two light beams differing in frequency by $\sim 1332 \text{ cm}^{-1}$, both incident on the diamond crystal along [001] and polarized along $[1\bar{1}0]$. The driving beams were ~ 20 -nsec pulses at $\lambda_1 = 7460 \text{ Å}$ and $\lambda_2 = 8285 \text{ Å}$ generated by stimulated Raman scattering¹⁰ (SRS) of Q-switched 6943-Å ruby laser light in a benzene oscillator cell⁸ and a liquid-nitrogen¹¹ amplifier cell, respectively. The fluorescence excitation was a collinear 3776-Å pulse derived from the same laser by second-harmonic generation and SRS, polarized along $[1\bar{1}0]$, and delayed to arrive at the crystal in coincidence with the driving pulses. Fluorescence was observed along $[110]$. Care was taken to attain nearly single transverse-mode generation of all the sources. The peak intensity of the pump beams was $(1-3) \times 10^8 \text{ W cm}^{-2}$; the 3776-Å excitation intensity was fixed at $\sim 1 \times 10^6 \text{ W cm}^{-2}$.

Coherent generation of $k \approx 0$ optical phonons by this technique has been reported previously and is well understood.⁹ From the measured Raman scattering cross section^{12,13} for the 1332 cm^{-1} line one calculates a peak SRS gain $\gamma = 2 \text{ cm}^{-1}$ at λ_2 for incident intensity $3 \times 10^8 \text{ W cm}^{-2}$ at λ_1 . The peak phonon power deposition P_p into the optical branch near $k = 0$ in terms of the intensity I_2 at λ_2 and the refractive index n is $P_p = \gamma I_2 \nu_p / n \nu_s$, or $3 \times 10^7 \text{ W cm}^{-3}$ for $I_2 = 3 \times 10^8 \text{ W cm}^{-2}$. The vibrational energy stored near $k = 0$ has a lower limit determined by an effective phonon lifetime equal to the inverse Raman scattering linewidth^{12,14} $\Delta \nu_s = 1.5 \text{ cm}^{-1}$; for $P_p = 3 \times 10^7 \text{ W cm}^{-3}$, the mini-

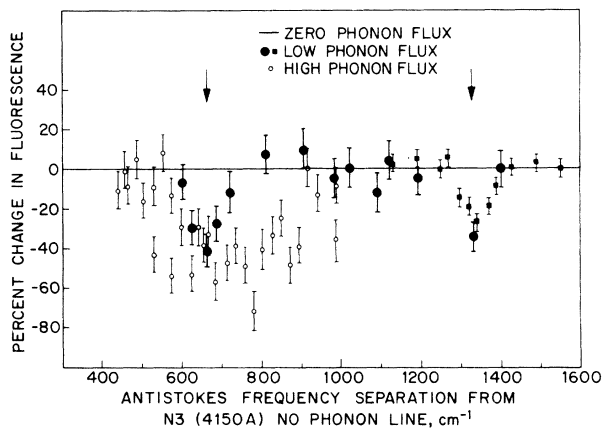


FIG. 2. Fractional change in fluorescence with optical phonon injection. Hole burning is observed at frequency separation of injected phonons (1332 cm^{-1}) and near subharmonic frequency.

mum stored energy is $3 \times 10^{-4}\text{ J cm}^{-3}$.

The effect of phonon injection on the anti-Stokes background fluorescence spectrum was measured between ν_0 and $\nu_0 + 1600\text{ cm}^{-1}$ with a scanning photomultiplier. Points on Fig. 2 showing the fractional change in fluorescence were obtained by averaging the results of 60 laser shots, with and without 1332-cm^{-1} phonon pumping, under fixed uv excitation conditions. The effect of the injected phonons is to reduce the fluorescence in a spectral region of $\pm 40\text{ cm}^{-1}$ centered at $\nu_0 + 1332 \pm 10\text{ cm}^{-1}$; as P_p was increased from 0 to 10^7 W cm^{-3} , the hole depth at $\nu_0 + 1332\text{ cm}^{-1}$ increased to 35%, roughly quadratically⁸ with P_p . It was carefully verified that hole burning did not occur in the absence of either the 7460- or 8285-Å driving beams; the hole burning was a function of $I_l I_S$ and independent of I_l/I_S .

Above a threshold $P_p \sim 10^7\text{ W cm}^{-3}$, the hole burned at $\nu_0 + 1332\text{ cm}^{-1}$ was accompanied by a second hole of width $\sim 80\text{ cm}^{-1}$ centered at $\nu_0 + 660 \pm 10\text{ cm}^{-1}$. At higher pumping intensities the second hole broadened asymmetrically, the center shifting to higher frequencies. Figure 2 shows observations near threshold and at the highest phonon flux, 10^8 W cm^{-3} , where the hole is centered near $\nu_0 + 770\text{ cm}^{-1}$.

From the spectrum and branching ratio of the nonthermal background fluorescence, together with the observations that (1) spectral hole burning occurs at frequencies separated from ν_0 by ν_p and $\nu_p/2$, (2) the hole widths are comparable to the no-phonon linewidth, and (3) the hole depth is a function only of $I_l I_S \sim P_p$, we conclude that (A) the background fluorescence is in large part hot

luminescence^{6,7} either of the $N3$ centers themselves or of neighboring centers which can readily exchange electronic excitation¹⁵ with $N3$ centers; and (B) the hole burning results in large part from direct (one-phonon) interaction with the luminescent centers of injected phonons¹⁶ at ν_p and secondary phonons near $\nu_p/2$.

To distinguish between fluorescence quenching and possible induced-absorption¹⁷ hole-burning mechanisms, a pulsed absorption spectrum was taken near $\nu_0 + \nu_p$ under the same phonon excitation conditions as above. In this experiment,⁸ absorption was found to account for a negligible fraction of the hole burning in Fig. 2.

The surprising observation that phonon injection quenches rather than enhances hot luminescence is difficult to explain on the basis of $N3$ -center fluorescence alone. Apparent quenching due to interference¹⁸ between hot luminescence and fluorescence enhanced by the injected phonons appears to be ruled out since the initial and final states for conceivable contributing processes are not identical. Quenching of hot luminescence from levels at $\nu_0 + \nu_p$ can in principle arise from nonradiative transitions $\nu_0 + \nu_p - \nu_0$, stimulated by the injected ν_p phonons. The importance of such processes can be estimated by comparing the injected phonon density with the lattice-mode density. From phonon dispersion data¹⁹ one estimates $N \approx 3 \times 10^{20}$ LO and TO modes in a bandwidth $\Delta\nu_s = 1.5\text{ cm}^{-1}$ at ν_p . On the basis of a phonon lifetime of 10^{-11} to 10^{-12} sec, only 5×10^{15} to 5×10^{16} phonons cm^{-3} are injected during the experiment. Even with the assumption that ν_p phonons may equilibrate with long lived²⁰ TA subharmonic terminal-state phonons near $\nu_p/2$ to give an effective lifetime as long as 10^{-8} sec, one estimates a maximum injected phonon density of $\sim 5 \times 10^{19}$ phonons $\text{cm}^{-3} < N$. We conclude that explanations based on stimulated one-phonon transitions within the vibronic manifold of the electronically excited $N3$ level appear to be unlikely.

The actual quenching mechanism is undoubtedly complex; however, several facts suggest that energy exchange with neighboring impurity sites may play a significant role. We note (1) the low quantum efficiency⁸ ($< 1\%$) for $N3$ fluorescence in our specimens, (2) the evidence from "edge" and x-ray excited luminescence²¹ for presence of centers with emission spectra including the hot-luminescence band, (3) the absence from the hot-luminescence spectra of characteristic one-phonon peaks, (4) that internal Auger processes are not expected to contribute to nonradiative decay,^{15,22}

and (5) the negative temperature dependence⁸ of the hot luminescence near 77°K. All of these observations are in fact consistent with neighboring sites as the origin of the hot luminescence; a quenching mechanism is then provided by phonon-assisted transport²³ of electronic excitation from a few such luminescing sites with energy $\nu_0 + \nu_p$ to a greater number of $N3$ sites with energy ν_0 . Spontaneous phonon-assisted transport is expected to be relatively ineffective because of the near-zero phonon group velocity and short phonon lifetime²⁴; the injected phonons, on the other hand, are driven coherently over the whole crystal.

Information about the $\nu_p/2$ subharmonic phonons is available from neutron dispersion data.¹⁹ Along principal symmetry directions the wavelength λ of 666 cm^{-1} TA and LA phonons falls in the range $4.6 < \lambda < 8.7 \text{ \AA}$. The mean free path of high- \vec{k} TA phonons at $T = 77^\circ\text{K} \ll T_D$ is expected to be boundary limited in perfect crystals²⁰; in our crystals containing²⁵ $\sim 10^{20}$ N atoms per cm^{-3} the lifetime may be considerably less as a result of TA \rightarrow LA conversion.

Coherent parametric acoustic phonon generation,¹ i.e., phonon breakdown, is expected to occur under our experimental conditions. The strength of the cubic anharmonicity is expressed by the Hamiltonian (1)

$$H = \sum_k [A(k)c_0c_k^\dagger c_{-k}^\dagger + \text{c.c.}], \quad (1)$$

where $A(k)$ is the anharmonic interaction constant, and c_0 , c_k are annihilation operators for pump and subharmonic phonons. In terms of the pump-phonon lifetime τ_0 , $|A|^2 = \pi\hbar^2 v_k (k^2 \tau_0 V)^{-1}$, where k and v_k are, respectively, the wave vector and effective velocity of the terminal phonons, and V the interaction volume. The critical pump-phonon density for phonon breakdown is

$$n_0/V = \hbar^2 (4\tau_k^2 |A|^2 V)^{-1} = k_1^2 \tau_0 (4\pi v_k \tau_k^2)^{-1},$$

which represents a threshold optical phonon power of $P_p = \hbar k^2 \omega_p (4\pi v_k \tau_k^2)^{-1}$. We note that P_p is independent of the optical phonon lifetime τ_0 , but strongly dependent on the acoustic phonon lifetime τ_k . For values $\tau_k = 10^{-8}$ sec (limited by the pulse duration), $v_k = 10^8 \text{ cm sec}^{-1}$, $k_1 = 10^8 \text{ cm}^{-1}$, and $\omega_p/2\pi c = 1332 \text{ cm}^{-1}$ we calculate a threshold $P_p(\text{calc})$ of $2 \times 10^5 \text{ W cm}^{-3}$ compared to the experimental value of $P_p(\text{exp}) \geq 10^7 \text{ W cm}^{-3}$. The latter is consistent with a lifetime $\tau_k \sim 10^{-9}$ sec or an acoustic phonon mean free path $\sim 10^{-3}$ cm.

These experiments demonstrate that strong buildup of acoustic subharmonic lattice vibrations

occurs at optical phonon excitation levels readily achieved by pulsed-laser SRS. The acoustic phonons produced ($4 < \lambda < 9 \text{ \AA}$) are well out in the Brillouin zone and are accessible to direct observation by x-ray diffraction. Analysis of the pumping threshold level suggests that phonon breakdown is in fact being observed. Our experiment also shows the feasibility of detecting phonons throughout the Brillouin zone by their effect on phonon-assisted fluorescence from suitable impurity centers.

We wish to acknowledge valuable discussions with Dr. R. Orbach, Dr. W. Kaiser, Dr. E. Mulazzi, Dr. K. Dransfeld, Dr. H. Mahr, and Dr. K. F. Renk, and thank K. W. Wecht for expert technical assistance. We are grateful for the use of several diamonds provided by the Diamond Research Laboratory, Johannesburg.

*Present address: Pierce Hall, Harvard University, Cambridge, Mass. 02138.

¹R. Orbach, Phys. Rev. Lett. **16**, 15 (1966), and IEEE Trans. Sonics Ultrason. **14**, 140 (1967).

²P. J. Dean, Phys. Rev. **139**, A588 (1965); P. A. Crowther and P. J. Dean, J. Phys. Chem. Solids **28**, 1115 (1967).

³E. V. Sobolev *et al.*, Fiz. Tverd. Tela **11**, 247 (1969) [Sov. Phys. Solid State **11**, 200 (1969)].

⁴See review P. J. Dean, in *Applied Solid State Science*, edited by R. Wolfe (Academic, New York, 1969), Vol. 1, p. 2.

⁵A. Halperin and O. Nawi, J. Phys. Chem. Solids **28**, 2175 (1967).

⁶V. Hizhnyakov and I. Tehver, Phys. Status Solidi **21**, 755 (1967), and **39**, 67 (1970).

⁷K. Peuker and E. D. Trifonov, Phys. Status Solidi **30**, 479 (1968).

⁸M. J. Colles and J. A. Giordmaine, to be published.

⁹J. A. Giordmaine and W. Kaiser, Phys. Rev. **144**, 676 (1966).

¹⁰See review by N. Bloembergen, Amer. J. Phys. **35**, 989 (1967).

¹¹J. B. Grun, A. K. McQuillan, and B. P. Stoicheff, Phys. Rev. **180**, 61 (1969).

¹²A. K. McQuillan, W. R. L. Clements, and B. P. Stoicheff, Phys. Rev. A **1**, 628 (1970).

¹³S. A. Solin and A. K. Ramdas, Phys. Rev. B **1**, 1687 (1970).

¹⁴F. Stenman, J. Appl. Phys. **40**, 4164 (1969).

¹⁵See review by P. T. Landsberg, Phys. Status Solidi **41**, 457 (1970).

¹⁶The SRS technique has the effect not only of injecting phonons but also of generating a local electric field (~ 10 esu) at the luminescent center, as a result of the local nonlinear electronic polarizability of the center itself. While contributions to the 1332- cm^{-1} hole burning due to electric-field-induced transitions cannot be completely ruled out, the purely electronic nonlinearity

is too small to generate a significant electric field at 660 cm^{-1} . We are therefore led to conclusion (B).

¹⁷W. J. Jones and B. P. Stoicheff, Phys. Rev. Lett. **13**, 657 (1964).

¹⁸U. Fano, Phys. Rev. **124**, 1866 (1961); D. L. Rousseau and S. P. S. Porto, Phys. Rev. Lett. **20**, 1354 (1968).

¹⁹J. L. Warren *et al.*, Phys. Rev. **158**, 803 (1967); R. Wehner *et al.*, Solid State Commun. **5**, 307 (1967).

²⁰R. Orbach and L. A. Vredevoe, Physics (Long Is.

City, N. Y.) **1**, 92 (1964).

²¹P. J. Dean, Phys. Rev. **139**, A588 (1965).

²²D. F. Nelson, J. D. Cuthbert, P. J. Dean, and D. G. Thomas, Phys. Rev. Lett. **17**, 1262 (1966).

²³M. Trlifaj, Czech. J. Phys. **6**, 533 (1956).

²⁴L. Genzel, in *Optical Properties of Solids*, edited by S. Nudelman and S. S. Mitra (Plenum, New York, 1969), p. 453.

²⁵W. Kaiser and W. L. Bond, Phys. Rev. **115**, 857 (1959).

Long-Wavelength Magnons in Heavy Rare Earths: Free or Frozen Lattice?*

D. T. Vigen and S. H. Liu

Institute for Atomic Research and Department of Physics, Iowa State University, Ames, Iowa 50010

(Received 12 April 1971)

We show that in the long-wavelength region the magnetoelastic effect allows both the free-lattice and the frozen-lattice mode to exist in the heavy rare earths Tb and Dy. The former may be more easily detected by ferromagnetic resonance at low frequencies and low temperatures, and the latter predominates at high frequencies and high temperatures.

There is strong magnetoelastic interaction in the heavy rare earths Tb and Dy as evidenced by the large lattice distortions in the ordered magnetic phases.¹⁻³ It has been suggested that this interaction is responsible for the ferromagnetic-to-helical ordering transition in these materials.^{4,5} One would naturally expect this interaction to manifest itself in the magnon spectrum. Turov and Shavrov⁶ argued that when a long-wavelength magnon is excited in the ferromagnetic phase, the lattice strain does not follow the precession of the spins. Therefore, enough energy must be supplied to the spins in order to pull them away from the strain axis. This results in a larger magnon energy gap than that due to the magnetic anisotropy alone. Cooper⁴ suggested that the lattice strain could follow the spins, so the magnon energy gap would be entirely due to the anisotropy. He showed by detailed numerical calculation that the contrast in behavior between the free-lattice and the frozen-lattice magnon modes becomes more acute when a magnetic field is applied in the hard direction in the basal plane. When the field is just strong enough to overcome the anisotropy field, the free-lattice-mode gap would be reduced to zero, whereas the frozen-lattice-mode gap would remain finite. This should allow a definitive test of the two theories by ferromagnetic resonance experiments. The experiments reported so far are controversial.⁷⁻¹¹ Generally speaking, the experiments performed at high frequencies (100 GHz) proved conclusively

the validity of the frozen-lattice model,⁹⁻¹¹ while the low-frequency experiments (10 GHz) gave somewhat dubious indications that the free-lattice mode might exist. Neutron-diffraction experiments supported the frozen-lattice model.¹²

We report here our theoretical study on the influence of the magnetoelastic interaction on the long-wavelength magnon energies. The microscopic local-interaction model proposed by Evenson and Liu⁵ is particularly suited for this study. This model assumes one or two ion interactions as in the macroscopic theory of Callen and Callen¹³ but allows the spin functions to couple to the local lattice distortions. A consequence of this model is that when the spins are aligned ferromagnetically, the lattice distortion is in agreement with the macroscopic theory; while in the helical spin configuration there is a periodic lattice distortion within a surface layer of the material, and the bulk of the material remains uniformly strained. This gives a microscopic justification of the lattice-clamping effect of Cooper.⁴ The skin depth for the periodic lattice distortion is measured by the inverse of the wave vector of the spin alignment.

The same idea applies when a spin wave is excited. When a spin precesses around its equilibrium position, it tends to drag the lattice distortion with it. For an infinite-wavelength magnon the lattice distortions of all the cells move in phase, so that add up to a macroscopic strain which follows the motion of the spins. However,